Equilibrium Geometries, Stabilities, and Electronic Properties of the Bimetallic Ag_2-doped Si_n ($n = 1-11$) Clusters: A Density-Functional Investigation

Ya-Ru Zhao[a], Xiao-Yu Kuang[a,b], Su-Juan Wang[a], Yan-Fang Li[a], and Peng Lu[a]

[a] Institute of Atomic and Molecular Physics, Sichuan University, Chengdu 610065, China
[b] International Centre for Materials Physics, Academia Sinica, Shenyang 110016, China

Reprint requests to X.-Y. K.; E-mail: scu_kxy@163.com

Z. Naturforsch. **66a,** 353 – 362 (2011); received May 10, 2010 / revised September 9, 2010

An ab initio method based on the density functional theory has been employed to investigate the behaviours of the bimetallic Ag_2-doped silicon clusters at a size of $n = 1-11$. The possible geometrical configurations, growth-pattern behaviours, stabilities, energy gaps, and electronic properties are presented and discussed. The optimized geometries reveal that the silicon atom surface-capped and silver atom substituted 3D structures are dominant growth patterns. The calculated averaged binding energy, fragmentation energy, and the second-order difference of energy manifest that the most stable structures of Ag_2Si_n ($n = 1-11$) clusters are Ag_2Si_2 and Ag_2Si_5 isomers, which is in qualitative agreement with the $AgSi_n$ clusters. In addition, the gap between highest occupied and lowest unoccupied molecular orbital (HOMO-LUMO) exhibits that the Ag_2Si_3 and Ag_2Si_5 isomers have dramatically enhanced chemical stability. Natural population analysis shows that the charge-transfer phenomena are coincidence with the $AgSi_n$ clusters but different from Mo_2Si_n systems. Furthermore, the dipole moments of stable Ag_2Si_n ($n = 1-11$) display a pronounced odd-even oscillation with the number of silicon atoms.

Key words: Ag-Si Cluster; Geometric Configuration; Density Function Method.

1. Introduction

Semiconductor Si_n clusters have attracted great attention and have been studied extensively by theoretical and experimental techniques because of their bulk crystalline fragments, as evidenced by the existence of 'magic number' effects in their physical and chemical properties [1 – 4]. However, pure silicon clusters are unsuitable as building block, because they are chemical reactive owing to the existence of their dangling bonds [5,6]. After a transition metal (TM) is doped into the silicon clusters, the TM:Si_n clusters tend to form closed-shell electronic structures that show the extraordinary stabilities compared with the pure species. Furthermore, the superconductivity, magnetism, charge-transfer, and other properties of TM-doped silicon are different from those of silicon clusters and bulk systems. Due to the unique properties, the behaviours of small transition metal silicon cluster have been widely investigated in recent years [7 – 13].

Several experimental projects of these metal-silicon clusters have been performed recently. Beck and Hiura have reported experimental investigations of small mixed transition metal silicon cluster in a pioneering mass spectrometric investigation using a laser vapourization technique [14 – 16]. Scherer et al. have produced mixed TM-silicon cluster by time-of-flight mass spectroscopy and studied the electronic states of CuSi, AgSi, and AuSi dimers by measuring their laser absorption spectra as well as by theoretical calculations using the CASPT2 method [17 – 20]. In addition, the VSi and NbSi dimers have been investigated by matrix-isolated electron spin resonance spectroscopy (ESP) spectroscopy while bond energies are detected experimentally [21 – 23]. Under the motivation of experimental results, some metal-silicon clusters calculations have also been performed by many different theoretical methods. For example, multireference couple-pair approximation (MRCPA) study on neutral CuSi [24]; complete active space self-consistent field (CASSCF) on MSi (M = Cu, Ag, Au) [6, 7]; density functional theory (DFT), second-order Møller-Plesset (MP2) perturbation theory, quadratic configuration interaction including single and double excitation (QCISD), and CASSCF followed by perturbation evaluation (CASPT2) on MSi, MSi^+, and MSi^-

Table 1. Geometries, symmetries, HOMO, LOMO, HOMO-LOMO gaps, vibration frequencies, and electron states of the stable Ag_2Si_n ($n = 1-11$) clusters.

Isomer	Symmetry	HOMO (Hartree)	LOMO (Hartree)	Energy Gap (eV)	Frequency (cm^{-1})	State
1a	$\boldsymbol{C_{2v}}$	**−0.19908**	**−0.12210**	**2.095**	**47.5, 241.7, 293.0**	$\mathbf{^1A_1}$
1b	$D_{\infty h}$	−0.13469	−0.11676	0.488	92.5, 135.2, 411.7, 757.9	–
2a	$\boldsymbol{C_{2v}}$	**−0.18922**	**−0.09611**	**2.534**	**45.4, 114.6, 157, 185.4, 206.2**	$\mathbf{^1A_1}$
2b	$C_{\infty v}$	−0.18165	−0.13752	0.201	45.7, 45.8, 100.4, 115.9, 300.4	$^3\Sigma$
2c	D_{2h}	−0.17337	−0.14183	0.858	75.4, 80.8, 183.7, 204.8,238.1	^1A_g
3a	C_{2v}	−0.21456	−0.11679	2.660	32.2, 85.8, 88.7, 133.0, 143.7	$^1A_1$
3b	$D_{\infty v}$	−0.18118	−0.15092	0.823	16.6, 34.3, 101.6, 107.5, 277.5	$^3\Sigma$
3c	$\boldsymbol{C_{2v}}$	**−0.21755**	**−0.11382**	**2.823**	**41.4, 42.3, 123.5, 132, 186.6**	$\mathbf{^1A_1}$
3d	C_s	−0.21463	−0.11672	2.664	32.0, 85.8, 88.4, 133.0, 143.9	$^1A'$
4a	$\boldsymbol{C_1}$	**−0.21558**	**−0.12191**	**2.549**	**35.0, 48.7, 91.3, 127.7, 154.0**	$\mathbf{^1A}$
4b	C_{2h}	−0.21783	−0.16650	1.397	22.0, 51.0, 58.7, 60.0, 117.0	^3B_u
4c	C_{2v}	−0.20625	−0.16715	1.064	31.0, 49.2, 55.5, 60.1, 115.4	$^3B_1$
4d	C_1	−0.20737	−0.11239	2.585	32.0, 48.0, 79.7, 121.6, 157.4	^1A
5a	D_{5h}	−0.20210	−0.15128	1.383	105.4, 114, 119.5, 125.7, 148.7	$^1A_1'$
5b	D_{2h}	−0.19996	−0.11011	2.445	36.6, 53.7, 84.8, 99.1, 99.8	^1A_g
5c	$\boldsymbol{C_1}$	**−0.21722**	**−0.10769**	**2.980**	**8.7, 25.4, 89.3, 107.3, 129.4**	$\mathbf{^1A}$
5d	C_1	−0.18964	−0.15671	0.896	43.5, 48.3, 59.2, 106.3, 110.5	^3A
6a	$\boldsymbol{C_s}$	**−0.22061**	**−0.11580**	**2.852**	**50.6, 51.1, 72.8, 82.3, 87.9**	$\mathbf{^1A}$
6b	C_1	−0.20724	−0.13899	1.857	52.4, 52.9, 75.8, 91.0, 118.5	^3A
6c	C_1	−0.19749	−0.12437	1.990	4.6, 60.1, 66.5, 77.2, 87.1	^1A
6d	C_1	−0.19936	−0.13079	1.866	49.8, 55.9, 74.2, 89.9, 109.3	^1A
7a	$\boldsymbol{C_1}$	**−0.21004**	**−0.13130**	**2.143**	**45.7, 58.8, 62.3, 74.0, 78.3**	$\mathbf{^1A}$
7b	C_1	−0.20557	−0.13311	1.972	35.4, 43.1, 56.8, 63.3, 79.7	^1A
7c	C_1	−0.19639	−0.12873	1.841	52.5, 54.8, 67.2, 94.1, 100.5	^1A
7d	C_1	−0.20086	−0.13748	1.725	36.5, 48.3, 68.0, 80.3, 84.9	^1A
8a	$\boldsymbol{C_1}$	**−0.21734**	**−0.13052**	**2.362**	**42.6, 51.4, 61.8, 76.4, 79.8**	$\mathbf{^1A}$
8b	C_1	−0.19980	−0.13933	1.645	32.0, 36.0, 58.4, 72.4, 82.0	^1A
8c	C_1	−0.20467	−0.15257	1.418	26.7, 39.9, 53.2, 58.9, 87.3	^1A
8d	C_1	−0.20708	−0.15018	1.548	37.9, 43.8, 63.4, 74.1, 88.2	^1A
8e	C_1	−0.21126	−0.12997	2.212	40.3, 47.1, 55.4, 59.2, 82.9	^1A
9a	$\boldsymbol{C_1}$	**−0.21345**	**−0.14187**	**1.948**	**44.4, 57.7, 70.3, 71.7, 87.6**	$\mathbf{^1A}$
9b	C_1	−0.21316	−0.14046	1.978	38.4, 60.3, 62.8, 68.5, 77.4	^1A
9c	C_1	−0.19896	−0.13049	1.863	32.5, 40.4, 50.2, 70.2, 82.2	^1A
9d	C_1	−0.20834	−0.14165	1.815	39.8, 43.4, 52.9, 69.8, 75.0	^1A
9e	C_1	−0.20888	−0.15195	1.549	25.2, 50.1, 64.6, 68.5, 79.7	^1A
10a	$\boldsymbol{C_1}$	**−0.22047**	**−0.13952**	**2.203**	**46.8, 51.3, 57.0, 70.2, 78.6**	^1A
10b	C_1	−0.21480	−0.14253	1.967	43.9, 58.6, 68.0, 72.9, 78.9	^1A
10c	C_1	−0.19925	−0.14817	1.390	31.3, 39.5, 44.7, 65.1, 71.6	^1A
10d	C_1	−0.20136	−0.13383	1.838	30.8, 32.7, 41.3, 66.9, 71.9	^1A
10e	C_1	−0.21884	−0.13986	2.149	36.4, 37.8, 53.9, 63.6, 65.1	^1A
10f	C_1	−0.20110	−0.13776	1.724	31.0, 39.8, 58.9, 64.3, 83.1	^1A
11a	C_1	−0.19146	−0.14063	1.383	41.8, 53.9, 66.9, 73.8, 81.0	^1A
11b	C_1	−0.21814	−0.14046	2.114	47.6, 59.9, 67.1, 76.2, 83.7	^1A
11c	C_1	−0.18474	−0.16026	0.666	22.7, 36.1, 48.6, 52.7, 66.9	^3A
11d	$\boldsymbol{C_1}$	**−0.20884**	**−0.14169**	**1.827**	**35.8, 38.0, 51.9, 71.5, 72.7**	$\mathbf{^1A}$
11e	C_1	−0.20587	−0.13912	1.816	28.1, 30.5, 51.1, 53.0, 60.2	^1A

(M = Cu, Ag, Au) [11 – 13]; DFT on MSi_n (M = Cr, Mo, W, Ir, Ag; $n = 1-6$) [21, 22, 25 – 27] and MSi_n (M = Re, Ta, Zr; $n = 1-12$) [3, 7] employing Gaussian 98 and ADF code.

For silver silicon clusters, different experimental and theoretical investigations have been undertaken for one silver atom doped silicon clusters [8, 19, 28, 29]. However, to our knowledge, there is no systematic theoretical investigation on the bimetallic Ag_2-doped silicon clusters until now. Will their structure and properties greatly differ from those of the $AgSi_n$ and Si_n clusters? To reveal the unusual properties of the bimetallic Ag_2-doped silicon clusters, the growth behaviours, equilibrium geometries, stabilities, HOMO–LUMO gaps and electronic properties are investigated and discussed in detail from a very small size to a relatively large size. Although a large numbers of possible initial isomers for each clusters size are extensively explored, we only list a few of the low-energy isomers in this paper. All of the structures reported here have position vibration frequencies and therefore correspond to the potential energy minima.

2. Computation Details

Our calculations of the Ag_2Si_n ($n = 1-11$) clusters with spin configurations considered are performed by using the Gaussian 03 program package [30] with the B3LYP exchange-correlation potential [31, 32] and an effective core potential (ECP) LanL2DZ basis set [33]. In the previous works, it has been demonstrated that the LanL2DZ basis set of the ECP theory are capable of providing results of very satisfactory and reasonable quality for the geometries, stabilities, and electronic properties of Si_n and TM: Si_n systems [7, 8, 11, 12, 34].

To test the reliability of our calculations, the bond length, vibration frequencies, and dissociation energies of the AgSi, Ag_2, and Si_2 molecules are calculated. The values of Ag−Si bond length (2.49 Å) and vibration frequency (272.4 cm^{-1}) are in good agreement with the experimental results (2.45 Å) and (297.0 cm^{-1}) [19, 29]. In addition, the bond lengths of Ag_2 and Si_2 molecular (2.611 Å and 2.35 Å) are close to the theoretical results (2.63 Å and 2.31 Å) and experimental results (2.53 Å and 2.25 Å) by Beutel [3, 4, 35, 36]. Due to the dependence of the calculated results on the pseudopotentials, this examination of bond lengths leads to deviations typically within 1 – 6%. Therefore, our study can be considered as preliminary and qualitative naturally.

3. Results and Discussions

3.1. Geometries and Growth Behaviours

Lots of possible initial structures, which include one-, two-, and three-dimensional configurations, have been considered in geometry optimizations, and all clusters are relaxed fully without any symmetry constraints. In our paper, the ground state isomer and few low-lying structures for each size are displayed in Figure 1 and their symmetry, HOMO, LUMO, HOMO-LUMO gaps, vibration frequencies, and electronic states are listed in Table 1.

Ag_2Si. According to the calculated results, it is found that the lowest-energy isomer is an acute-angle triangular structure (1a) with the singlet spin configuration and C_{2v} symmetry, a 79.0° angle and a 2.497 Å bond length. The linear $D_{\infty h}$ structure (1b) with singlet spin configuration is 1.572 eV higher in total energy than the 1a structure.

Ag_2Si_2. For the Ag_2Si_2 clusters, the opened trigonal pyramid structure (2a) with C_{2v} symmetry has the minimum total energy. When the Si atom is added to the 1b structure, the linear $C_{\infty v}$ structure (2b) is proved to be a stable structure. However, the 2b isomer has large relative energy compared with 2a. As shown in Figure 1, the planar Ag_2Si_2 isomer (D_{2h}) structure can be viewed as two silver atoms substituting two silicon atoms of the framework of Si_4 [37].

Ag_2Si_3. When two silicon atoms of the D_{3h} symmetry ground state of the Si_5 cluster are substituted by two silver atoms, the initial D_{3h} structure distorts to yield the trigonal bipyramidal C_{2v} Ag_2Si_3 model (3a). Similarly, the $D_{\infty v}$ linear structure (3b) with a $^3\Sigma$ state can be obtained from the 2b isomer by adding a silicon atom at symmetrical site. After a slight distortion of the trapezoidal planar C_{2v} structure, a house-like isomer (3c) is yielded. The calculated results indicated that the 3c isomer is the most stable structure of the Ag_2Si_3 cluster. As for the C_s structure (3d), it can be interpreted as a distorted geometry of the C_{2v} Ag_2Si_3 isomer.

Ag_2Si_4. Four possible isomers considering various spin states are optimized for the Ag_2Si_4 cluster. The distorted trigonal prism C_1 structure (4a), which is generated from two silver atoms substituting two silicon atoms of the distorted D_{3h} Si_6 cluster, is proved to be the most stable structure of the Ag_2Si_4 isomers. The planar C_{2h} and C_{2v} structures are also stable geometries while their stabilities are a bit lower than that of 4a. The additional low symmetry C_1 structure (4d) is a minimum of the potential surface which can be viewed as two silver atoms capping on the non-planar C_{2v} symmetry Si_4 cluster. According to the calculated results, the stability of 4d is weaker than that of 4a.

Ag_2Si_5. Guided by the Si_7 clusters, the pentagonal bipyramid D_{5h} (5a) isomer of the Ag_2Si_5 cluster can be obtained. In addition, the planar D_{2h} (5b) structure with singlet spin configuration is optimized to be a stable geometry. For the most stable structure, the 5c isomer can be interpreted as silver atom replacing a silicon atom of the trigonal prism Si_6 cluster and then

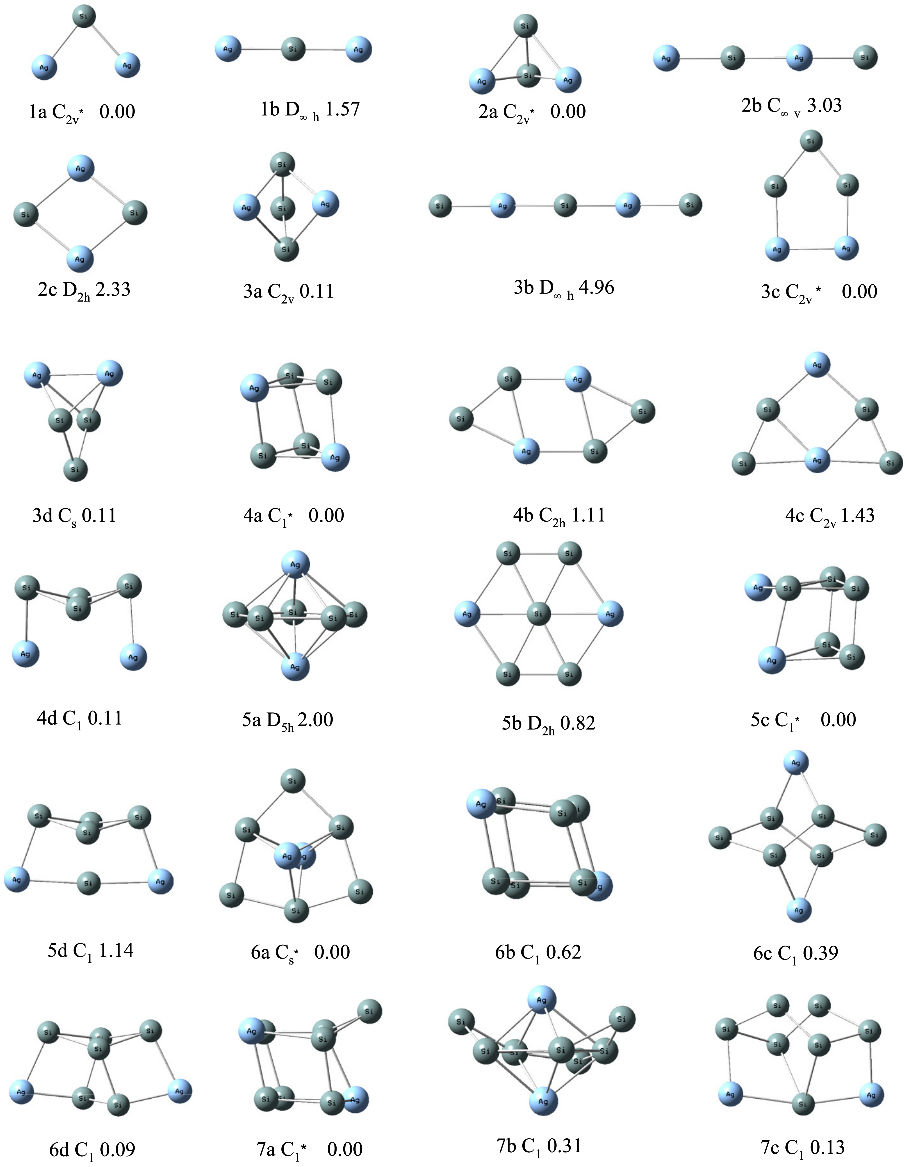

Fig. 1 (colour online). All equilibrium structures of the Ag_2Si_n ($n = 1-11$) clusters; the corresponding point-group symmetries along with relative stabilities (eV) are presented by the B3LYP calculation; the stars show the lowest-energy structures of Ag_2Si_n.

another silver atom tri-capping on this distorted prism of the $AgSi_5$ isomer. After one silicon atom is localized at the center site of the bottom of the Ag_2Si_4 4d isomer, the C_1 isomer (5d) with ^{3}A state is generated.

Ag_2Si_6. In the calculations, we find four different structures for the Ag_2Si_6 clusters with an energy range of 0.616 eV. The lowest-energy (6a) isomer is a distorted hexagon bi-pyramid structure. However, its D_{3h} symmetry is lowered to be the C_s symmetry due to the Jahn-Teller effect. When two silicon atoms are capped on the trigonal prism 4a structure, the distorted orthorhombic structure 6b isomer with ^{3}A state is yielded. The new star-like structure (6c) is optimized and proved to be a stable isomer. For the 6d structure, it can be viewed as one silicon atom added to the 5d structure of the Ag_2Si_5 isomer.

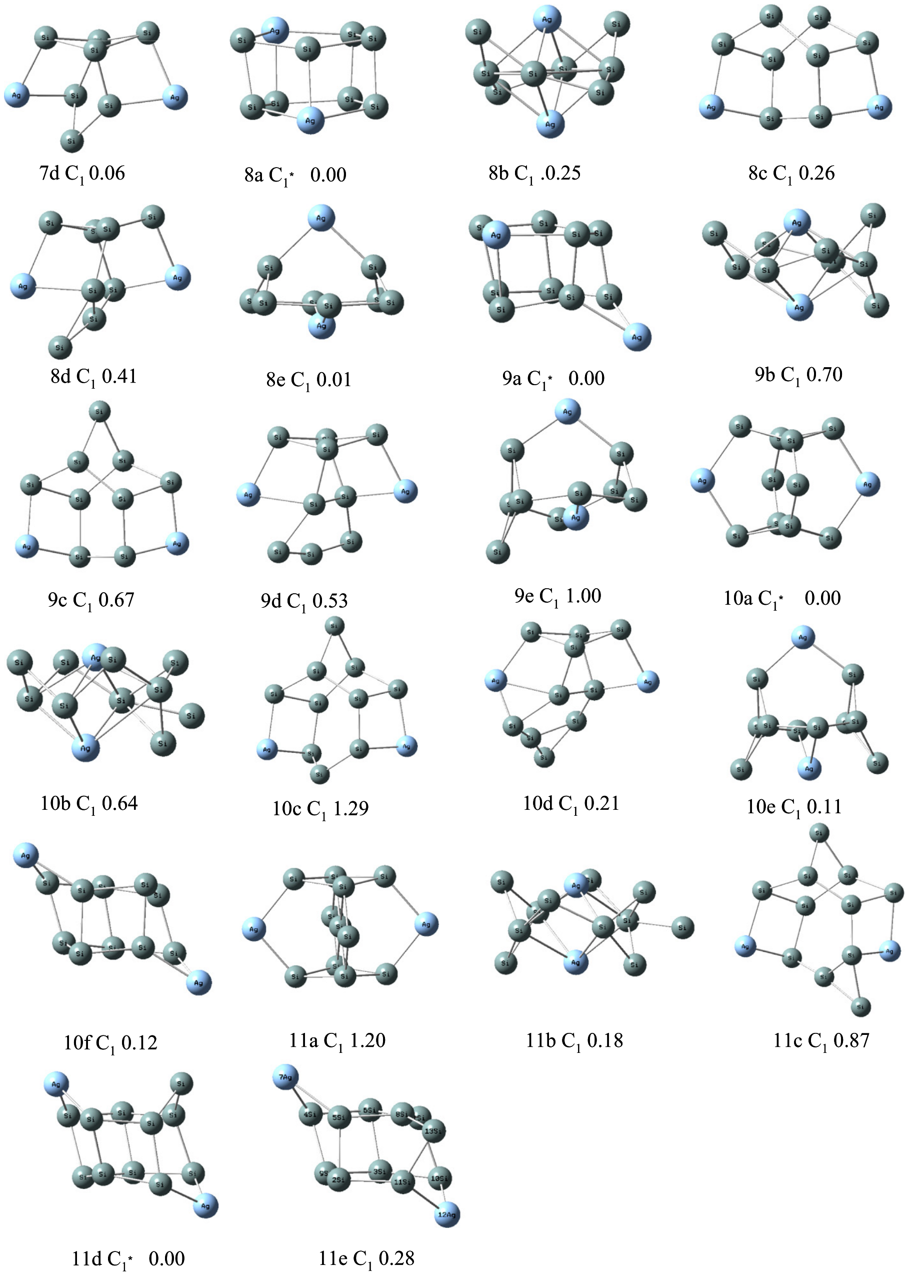

Fig. 1 (colour online). (continued).

Ag_2Si_7. Guided by the previous structures of Si_9 and Ag_2Si_n ($n = 1-6$) clusters, four possible Si_2Ag_7 geometries are optimized to be the local minima on the respective potential surfaces according to calculated frequency analysis. The lowest-energy 7a structure can be described as silicon atom capping on the 6b geometry. When two silicon atoms of the C_s symmetry Si_9 cluster [1] are substituted by two silver atoms, the C_1 symmetry Si_2Ag_7 structure (7b) is generated. Furthermore, the new isomer (7c) is obtained from two silicon atoms face-capping on the top of the 5d structure. The additional 7d geometry is optimized after one silicon atom is capped on the stable 6d structure of the Si_2Ag_6 cluster.

Ag_2Si_8. According to our calculation, Ag_2Si_8 isomers with high symmetries are proved to be the unstable structures. For example, when two silicon atoms of the D_{5h} symmetry Si_{10} cluster [2] are replaced by two silver atoms, the high symmetry is lowered to be the C_1 symmetry and a distorted pentagonal prism structure 8a is finally obtained. Similarly, the 8b isomer is a substituted structure from another Si_{10} cluster [4]. The 8c and 8d isomers emerge from one silicon atom being added to the 7c and 7d isomers, respectively. It is interesting to point out that the 8e structure is obtained from the 10e isomer by removing two silicon atoms.

Ag_2Si_9. The most stable Ag_2Si_9 geometry (9a) is a derivative structure of the 8a isomer. It is generated from one silver atom of the 8a structure substituted by a silicon atom and then the replaced silver atom is surface bi-capped on the new distorted pentagonal prism $AgSi_9$ structure. Similar to the Ag_2Si_8 isomers, the low-lying structures 9b, 9c, 9d, and 9e are obtained from silicon atoms added to the 8b, 8c, 8d, and 8e isomers, respectively.

Ag_2Si_{10}. Guided by the Ag_2Si_9 structures, it is interesting to find the 10a and 10e isomers being two derivatives from 9e with the second silver atom connecting dissimilar silicon atoms. Therefore, a bit relative energy (0.109 eV) exists between 10a and 10e isomers. After a silicon atom capping on the stable 9b, 9c, and 9d structures, respectively, the low-lying Ag_2Si_{10} isomers 10b, 10c, and 10d are generated. The 10f isomer appears when the tenth silicon atom is inserted into the 9a structure in the same way as the ninth silicon atom.

Ag_2Si_{11}. For $n = 11$, one equilibrium 11a structure is formed with one silicon atom being inserted into the center of the most stable 10a isomer. Additionally, the 11b and 11c isomers are yielded from 10b and 10c Ag_2Si_{10} clusters. The stable 11d and 11e isomers can be viewed as two derivatives of the 10f isomer after a silicon atom bi-capping on the different sites of the 10f geometry. Comparing the total energies, it is found that the 11d cluster is the lowest-energy structure for the Ag_2Si_{11} cluster.

On the basis of the detailed analysis of the small-sized Ag_2Si_n ($n = 1-11$) clusters, it is concluded that the silicon atom surface-capped and silver atom substituted structures are the dominant structures of all the isomers. In addition, the lowest-energy isomers are 3D structures from silicon size $n = 2$ to 11 expect for the Ag_2Si_3 structure.

3.2. Relative Stability

In order to predict relative stabilities of the most stable Ag_2Si_n ($n = 1-11$) clusters, it is significant to investigate the averaged atomic binding energy $E_b(n)$, the fragmentation energy $D(n,n-1)$, and the second-order difference of energy $\Delta_2E(n)$, which are defined as follows:

$$E_b(n) = \frac{2E(\mathrm{Ag}) + nE(\mathrm{Si}) - E(\mathrm{Ag_2Si}_n)}{n+2}, \quad (1)$$

$$D(n,n-1) = E(\mathrm{Ag_2Si}_{n-1}) + E(\mathrm{Si}) - E(\mathrm{Ag_2Si}_n), \quad (2)$$

$$\Delta_2E(n) = E(\mathrm{Ag_2Si}_{n-1}) + E(\mathrm{Ag_2Si}_{n+1}) - 2E(\mathrm{Ag_2Si}_n), \quad (3)$$

where $E(\mathrm{Ag_2Si}_{n-1})$, $E(\mathrm{Si})$, $E(\mathrm{Ag})$, $E(\mathrm{Ag_2Si}_n)$, and $E(\mathrm{Ag_2Si}_{n+1})$ denote the total energies of the Ag_2Si_{n-1}, Si, Ag, Ag_2Si_n, and Ag_2Si_{n+1} clusters, respectively. The calculated $E_b(n)$, $D(n,n-1)$, and $\Delta_2E(n)$ values of the most stable Ag_2Si_n isomers are listed in Table 2 and the relative curves of $E_b(n)$, $D(n,n-1)$, and $\Delta_2E(n)$ against the corresponding number of the silicon atoms are plotted in Figure 2. As seen from the figure, the atomic averaged binding energy shows a smooth growing trend with increasing size. Two peaks are found at $n = 2$ and 5, indicating that the Ag_2Si_2 and Ag_2Si_5 isomers are relatively more stable. In addition, it is found that the two curves of $D(n,n-1)$ and $\Delta_2E(n)$ show a similar tendency with the change of silicon atom number, which indicates that the predicted relative stabilities of the Ag_2Si_n clusters vary synchronously with the cluster size. In both of the curves, two remarkable

Table 2. Calculated averaged atomic binding energy $E_b(n)$, fragmentation energy $D(n,n-1)$, and second-order difference of energy $\Delta_2E(n)$ of the most stable Ag_2Si_n ($n = 1-11$) clusters (unit: eV).

Size (n)	1	2	3	4	5	6	7	8	9	10	11
$E_b(n)$	1.120	1.717	1.878	2.030	2.221	2.253	2.277	2.357	2.434	2.474	2.489
$D(n,n-1)$	–	3.507	2.522	2.790	3.368	2.477	2.468	3.081	3.202	2.913	2.667
$\Delta_2E(n)$	–	0.986	−0.269	−0.577	0.891	0.009	0.613	−0.121	0.288	0.245	–

peaks at $n = 2$ and 5 for the Ag_2Si_n clusters are also found.

This hints that the corresponding Ag_2Si_2 and Ag_2Si_5 clusters have slightly stronger relative stabilities as compared to their neighbours. Moreover, it is worthy to point out that this feature of relative stability on the bimetal Ag_2-doped silicon clusters is in qualitatively agreement with the single silver atom doped silicon clusters [8].

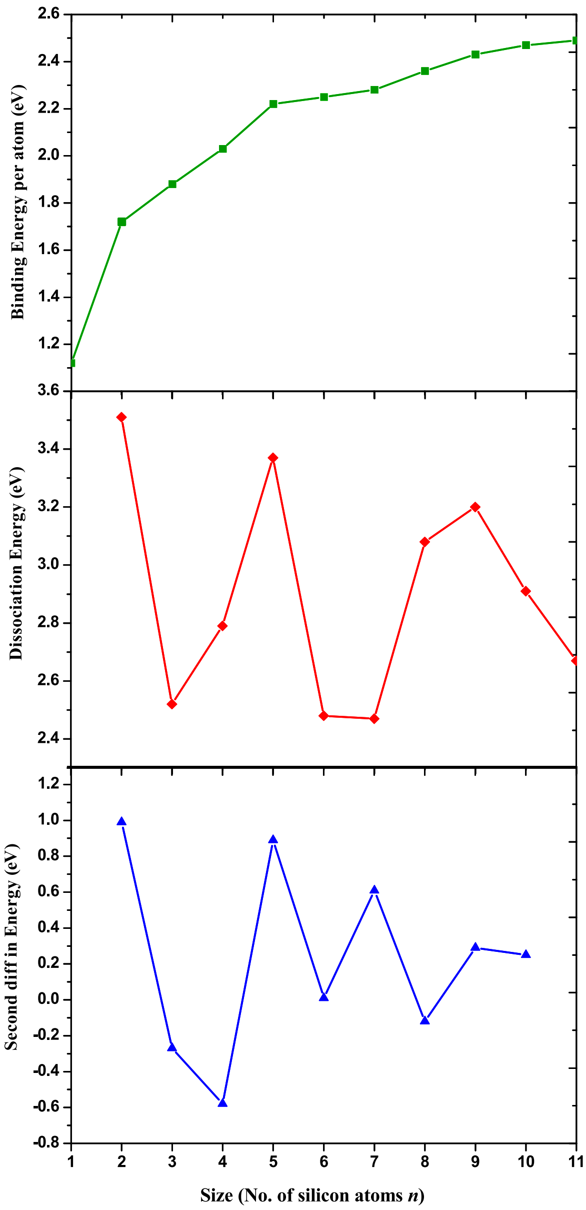

Fig. 2 (colour online). Atomic averaged binding energies, fragmentation energies, and second-order difference of energies for Ag_2Si_n isomers as a function of clusters size.

3.3. HOMO-LOMO gap

The electronic properties of the Ag_2Si_n ($n = 1-11$) clusters are discussed by examining the energy gap between the highest occupied molecular orbital (HOMO) and lowest unoccupied molecular orbital (LUMO). The HOMO-LUMO energy gap reflects the ability of electrons to jump from occupied orbitals to unoccupied orbitals, which represents the ability of the molecule to participate into chemical reactions in some degree. A large value of the HOMO-LUMO energy gap is related to an enhanced chemical stability, contrarily, a small one corresponds to a high chemical activity. Here, the HOMO and LUMO energies as well as the corresponding HOMO-LUMO gaps for each Ag_2Si_n cluster are tabulated in Table 1 and the calculated HOMO-LUMO gaps for the most stable isomers at each size are plotted as curves in Figure 3. Comparing with the previous works, we find that the energy gaps of the most stable Ag_2Si_n clusters are bigger than those of the MSi_n (M = Ta, Yb, Ni) and Mo_2Si_n clusters [34], which may be caused by the electronic shell closure of the silver atoms. This effect was demonstrated by small even sized silver and copper clusters experimentally and by copper clusters theoretically [38]. It seems worthwhile to note that the energy gaps of Ag_2Si_3 and Ag_2Si_5 isomers are higher than those of their neighbours, which means that the corre-

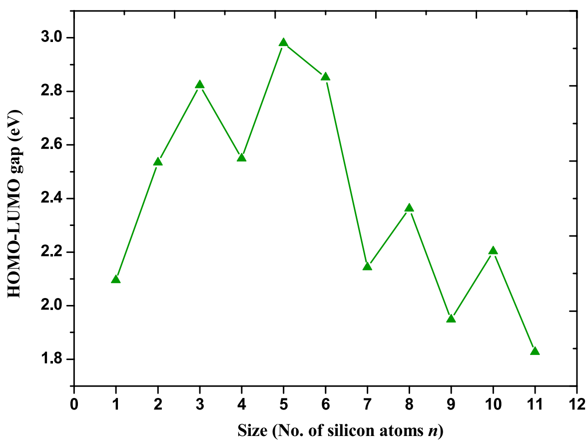

Fig. 3 (colour online). Size dependence of the HOMO-LUMO gaps for the lowest-energy structures of Ag_2Si_n clusters.

sponding clusters have dramatically enhanced chemical stability. Therefore, the Ag_2Si_5 cluster can be seen as the most stable building block and can be selected as candidate of novel nanomaterials. Unfortunately, the chemical stability of the most relative stable Ag_2Si_2 isomer is weaker than that of the Ag_2Si_3 and Ag_2Si_5 isomers.

3.4. Population Analysis and Dipole Moments

Natural population analysis on the MSi_n clusters can provide reliable charge-transfer information. Therefore, the natural populations (NPs) of the different silver atoms in the most stable Ag_2Si_n systems are listed in Table 3. As shown in the table, the NP values of the silver atoms for Ag_2Si_n ($n = 1-11$) clusters are positive, indicating that the charge in the corresponding cluster transfer from silver atoms to the Si_n frames owing to a larger electronegativity of the silicon than that of the silver atom. This feature is in agreement with $AgSi_n$ clusters but different from Mo_2Si_n systems. In addition, the natural electronic configuration for the silver atom in the most stable Ag_2Si_n systems is tabulated in Table 4. According to the calculated results, there are 0.08 – 0.41 e charges transferred from 5*s* and 4*d* orbitals to 5*p* and 6*p* orbitals for a silver atom in different Ag_2Si_n clusters. In the different isomers, it is seen that the number of occupying 4*d* electrons assigned on each silver atom in the different isomers is more than 9.89 e, which indicates that the 4*d* orbitals of the silver atoms in the Ag_2Si_n cluster are dominant core orbitals.

Table 3. Dipole moment of the lowest-energy Ag_2Si_n ($n = 1-11$) clusters, natural charges populations of the different silver atoms of Ag_2Si_n systems, where Ag (1) and Ag (2) correspond to the top (or left) silver and bottom (or right) silver atoms in Figure 1.

Isomer	Dipole moment (D)	Natural charges populations Ag (1)	Natural charges populations Ag (2)
Ag_2Si	1.896	0.0480	0.0480
Ag_2Si_2	3.465	0.2551	0.2551
Ag_2Si_3	4.277	0.2049	0.2049
Ag_2Si_4	3.299	0.2935	0.2933
Ag_2Si_5	3.935	0.2696	0.2493
Ag_2Si_6	0.207	0.3386	0.3386
Ag_2Si_7	0.744	0.2878	0.3210
Ag_2Si_8	0.729	0.2250	0.3344
Ag_2Si_9	3.219	0.1928	0.4640
Ag_2Si_{10}	0	0.3504	0.3504
Ag_2Si_{11}	1.635	0.4348	0.3484

Table 4. Natural electronic configurations of the silver atoms in the most stable Ag_2Si_n systems, where the Ag (1) and Ag (2) correspond to the top (or left) silver and bottom (or right) silver atoms in Figure 1.

Isomer	Ag (1) 5*s*	Ag (1) 4*d*	Ag (1) 5*p*	Ag (1) 6*p*	Ag (2) 5*s*	Ag (2) 4*d*	Ag (2) 5*p*	Ag (2) 6*p*
Ag_2Si	0.94	9.93	0.08	0	0.94	9.93	0.08	0
Ag_2Si_2	0.70	9.94	0.10	0.01	0.70	9.94	0.10	0.01
Ag_2Si_3	0.74	9.94	0.13	0	0.74	9.94	0.13	0
Ag_2Si_4	0.65	9.91	0.14	0.01	0.65	9.91	0.14	0.01
Ag_2Si_5	0.63	9.91	0.19	0.01	0.62	9.91	0.22	0.01
Ag_2Si_6	0.36	9.90	0.40	0.01	0.36	9.90	0.40	0.01
Ag_2Si_7	0.60	9.90	0.21	0.01	0.58	9.90	0.19	0.01
Ag_2Si_8	0.60	9.90	0.27	0.01	0.56	9.90	0.20	0.01
Ag_2Si_9	0.65	9.89	0.27	0.01	0.52	9.92	0.10	0.01
Ag_2Si_{10}	0.60	9.92	0.13	0.01	0.60	9.92	0.13	0.01
Ag_2Si_{11}	0.53	9.91	0.12	0	0.61	9.90	0.14	0

As we known, the dipole moment can reflect the electronic cloud of the specific cluster in the presence of the external static electric field. The dipoles of the most stable Ag_2Si_n ($n = 1-11$) clusters are listed in Table 3. As shown in the table, the values of the dipole moments are within 0 – 4.227 D and the values of Ag_2Si_3 and Ag_2Si_5 isomers are larger than the others. This finding is in agreement with the large energy gaps of the Ag_2Si_3 and Ag_2Si_5 isomers, which may indicate that there exists a relationship between the dipole moment and the HOMO-LUMO energy gap. In this case, the dipole moments for the most stable isomers at each size are plotted as curves in Figure 4. It is found that the dipole moments exhibit odd-even alternative behaviour when $n > 1$, indicating that odd-numbered

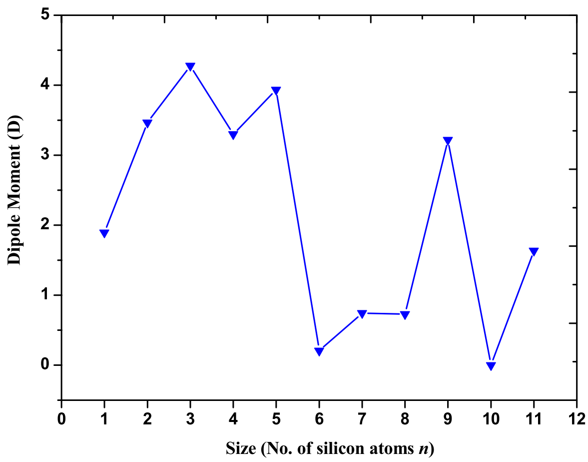

Fig. 4 (colour online). Size dependence of the dipole moments for the lowest-energy structures of Ag_2Si_n clusters.

Ag_2Si_n clusters have a relatively higher dipole moment than the neighbouring even-numbered sizes. When $n = 1-6$, the curve shows the similar tendency as the HOMO-LUMO gaps (Fig. 3), while the contrary tendency displays when $n = 7-11$. It can be expected that the dipole moment of the Ag_2Si_n isomers are mainly dependent on a symmetric distribution of the silicon atoms around two silver atoms. For example, Ag_2Si_5 and Ag_2Si_9 isomers have higher dipole moments because the distribution of odd-numbered silicon atoms around the silver atoms in 5c and 9a isomers is unsymmetrical. On the contrary, the dipole moment of the Ag_2Si_{10} isomer is zero due to a symmetric distribution of the silicon atoms around the silver atoms.

4. Conclusion

The growth behaviours, stabilities, HOMO-LOMO energy gaps, population analysis, and dipole moments of the Ag_2Si_n ($n = 1-11$) clusters are investigated theoretically at the B3LYP level employing LanL2DZ basis sets. All the calculated results are summarized as follows:

(i) The optimized geometries reveal that the silicon atom surface-capped and silver atom substituted structures are dominant structures in the growth behaviours and the lowest-energy isomers are 3D structures except the Ag_2Si_3 structure.

(ii) According to the averaged atomic binding energy, the fragmentation energy, and the second-order difference of energy analyses of the most stable Ag_2Si_n clusters, it is concluded that the small Ag_2Si_2 and Ag_2Si_5 isomers are more stable than their neighbouring isomers.

(iii) Due to the electronic shell closure of the silver atoms, the energy gaps of most stable Ag_2Si_n clusters are bigger than those of the MSi_n (M = Ta, Yb, Ni) and Mo_2Si_n clusters. In addition, the HOMO-LOMO energies exhibit that the Ag_2Si_3 and Ag_2Si_5 isomers have dramatically enhanced chemical stability.

(iv) Based on the calculated natural population and the natural electronic configuration, it is noticed that the charges are transferred from silver atoms to the silicon atoms. Moreover, the dipole moments of the most stable isomers exhibit odd-even alternative behaviour when $n > 1$, indicating that odd-numbered Ag_2Si_n clusters have relatively higher dipole moments than the neighbouring even-numbered sizes.

Acknowledgements

This work was supported by the Doctoral Education Fund of Education Ministry of China (No. 20050610011) and the National Natural Science Foundation of China (No. 10974138).

[1] K. Raghavachari and C. M. Rohlfing, J. Chem. Phys. **89**, 2219 (1988).
[2] K. Raghavachari, J. Chem. Phys. **84**, 5672 (1986).
[3] P. Guo, Z. Y. Ren, F. Wang, J. Bian, J. G. Han, and G. H. Wang, J. Chem. Phys. **121**, 12265 (2004).
[4] K. P. Huber and G. Herzberg, Constants of Diatomic Molecular, Van Nostrand, New York 1997.
[5] I. Rata, A. A. Shvartsburg, M. Horoi, T. Frauenheim, K. W. Michael Siu, and K. A. Jackson, Phys. Rev. Lett. **85**, 546 (2000).
[6] F. Hagelberg, J. Leszczynski, and V. J. Murashov, Mol. Struct. (Theochem) **454**, 209 (1998).
[7] J. Wang and J. G. Han, J. Chem. Phys. **123**, 064306 (2005).
[8] P. F. Zhang, J. G. Han, and Q. R. Pu, J. Mol. Struct. (Theochem) **635**, 25 (2003).
[9] J. G. Han and F. Hagelberg, Chem. Phys. **263**, 255 (2001).
[10] C. Xiao, F. Hagelberg, and W. A. Lester, Phys. Rev. B **66**, 75425 (2002).
[11] J. G. Han and F. Hagelberg, J. Mol. Struct. (Theochem) **549**, 165 (2001).
[12] J. G. Han, Chem. Phys. **286**, 181 (2003).
[13] J. G. Han, C. Xiao, and F. Hagelberg, Struct. Chem. **13**, 173 (2002).
[14] S. M. Beck, J. Chem. Phys. **90**, 6306 (1989).
[15] S. M. Beck, J. Chem. Phys. **87**, 4233 (1987).
[16] H. Hiura, T. Miyaiima, and T. Kanayama, Phys. Rev. B **86**, 1733 (2001).
[17] J. J. Scherer, J. B. Paul, C. P. Collier, and R. J. Saykally, J. Chem. Phys. **102**, 5190 (1995).
[18] J. B. Paul, J. J. Scherer, C. P. Collier, and R. J. Saykally, J. Chem. Phys. **104**, 62782 (1996).
[19] J. J. Scherer, J. B. Paul, C. P. Collier, and R. J. Saykally, J. Chem. Phys. **103**, 113 (1995).
[20] J. J. Scherer, J. B. Paul, C. P. Collier, and R. J. Saykally, J. Chem. Phys. **103**, 9187 (1995).
[21] Y. M. Harrick and W. J. Weltner Jr., Chem. Phys. **94**, 3371 (1991).
[22] K. A. Gringerick, J. Chem. Phys. **50**, 5426 (1969).

[23] J. R. Kingcade Jr. and K. A. Gringerick, J. Chem. Soc. Faraday Trans. **285**, 195 (1989).
[24] M. Tomonari, Y. Mochizuki, and K. Tanaka, Theor. Chem. Acc. **101**, 332 (1999).
[25] A. Boldyrev, J. Simons, J. J. Scherer, J. B. Paul, C. P. Collier, and R. J. Saykally, J. Chem. Phys. **108**, 5728 (1998).
[26] P. Turski and M. Barysz, J. Chem. Phys. **111**, 2973 (1999).
[27] M. Abe, T. Nakajima, and K. Hirao, J. Chem. Phys. **117**, 7960 (2002).
[28] P. Turski, Chem. Phys. Lett. **315**, 115 (1999).
[29] P. Turski and M. Barysz, J. Chem. Phys. **113**, 4654 (2000).
[30] M. J. Frisch, G. W. Trucks, H. B. Schlegel, G. E. Scuseria, M. A. Robb, J. R. Cheeseman, J. A. Montgomery, Jr., T. Vreven, K. N. Kudin, J. C. Burant, J. M. Millam, S. S. Iyengar, J. Tomasi, V. Barone, B. Mennucci, M. Cossi, G. Scalmani, N. Rega, G. A. Petersson, H. Nakatsuji, M. Hada, M. Ehara, K. Toyota, R. Fukuda, J. Hasegawa, M. Ishida, T. Nakajima, Y. Honda, O. Kitao, H. Nakai, M. Klene, X. Li, J. E. Knox, H. P. Hratchian, J. B. Cross, V. Bakken, C. Adamo, J. Jaramillo, R. Gomperts, R. E. Stratmann, O. Yazyev, A. J. Austin, R. Cammi, C. Pomelli, J. Ochterski, P. Y. Ayala, K. Morokuma, G. A. Voth, P. Salvador, J. J. Dannenberg, V. G. Zakrzewski, S. Dapprich, A. D. Daniels, M. C. Strain, O. Farkas, D. K. Malick, A. D. Rabuck, K. Raghavachari, J. B. Foresman, J. V. Ortiz, Q. Cui, A. G. Baboul, S. Clifford, J. Cioslowski, B. B. Stefanov, G. Liu, A. Liashenko, P. Piskorz, I. Komaromi, R. L. Martin, D. J. Fox, T. Keith, M. A. Al-Laham, C. Y. Peng, A. Nanayakkara, M. Challacombe, P. M. W. Gill, B. G. Johnson, W. Chen, M. W. Wong, C. Gonzalez, and J. A. Pople, GAUSSIAN 03 (Revision E.01), Gaussian, Inc., Wallingford, CT, 2004.
[31] A. D. Becke, J. Chem. Phys. **98**, 5648 (1993).
[32] C. Lee, W. Yang, and R. G. Parr, Phys. Rev. B **37**, 785 (1988).
[33] W. R. Wadt and P. J. Hay, J. Chem. Phys. **82**, 284 (1985).
[34] J. G. Han, R. N. Zhao, and Y. H. Duan, J. Phys. Chem. A **111**, 2148 (2007).
[35] V. Bonacic-Koutecky, L. Cespiva, P. Fantucci, and J. Koutecky, J. Chem. Phys. **98**, 7981 (1993).
[36] V. Beutel, H. G. Kramer, G. L. Bhale, M. Kuhn, K. Weyers, and W. Demtröder, J. Chem. Phys. **98**, 2699 (1993).
[37] A. A. Shvartsburg, B. Liu, M. F. Jarrold, and K. M. Ho, J. Chem. Phys. **112**, 4517 (2000).
[38] I. Katakuse, T. Ichihara, Y. Fujita, T. Matsuo, T. Sakurai, and H. Matsuda, Int. J. Mass Spectrom. Ion Process. **67**, 229 (1985).